

# **Studies of changes in volume in right ventricle with electrical bio impedance**

Licentiate thesis

by

Karin Järverud



Stockholm 2002



## Abstract

---

In intracardiac impedance, electrical bio-impedance is measured inside the heart. This signal is known to reflect the volume of blood passing in and out of the ventricles. In transthoracic impedance the measurement current and voltage sensing is connected on the subject's chest. In this thesis, the intracardiac impedance is studied in general, and in the filling phase (diastole) in particular. The diastolic intracardiac impedance displays a consistent slope change (notch). The notch in the present thesis has similar features as the non-invasive transthoracic impedance O-wave reported earlier. The notch occurrence was found to be well comparable with results in work with O-wave. The notch was found closely after early rapid ventricular filling but before ventricular filling caused by atrial contraction and it is concluded that the notch is not caused by atrial contraction. The notch is most likely caused by cardiac wall movements in rapid ventricular filling. The observations in this thesis are made in two different data sets; in animals and in humans and with different types of intracardiac leads. The lead implantations were performed by several different physicians. With the consistent results from these two studies at hand, this licentiate thesis concludes that the diastolic intracardiac impedance notch is a characteristic of intracardiac impedance, that the notch is the intracardiac equivalent of the non-invasive transthoracic impedance O-wave and that it is a sensed physiological cardiac parameter of diastole. Since the present data is measured intracardially it can be concluded that the non-invasive O-wave in fact is caused by cardiac movements.

**Keywords:** intracardiac impedance, O-wave, diastole, pacing

## Preface

---

The present dissertation is submitted to the Karolinska Institutet, in partial fulfillment of the requirement for the degree of Licentiate of Medicine. The work has been done at Karolinska Institutet, Department of Medical Laboratory Science and Technology, Division of Medical Engineering, in the period 1998 – 2002.

### Acknowledgements

This thesis is financially supported by St Jude Medical AB.

I wish to express my deepest gratitude and appreciation to all those involved in this project. Without the important support from the following persons, this thesis would not have been possible.

Firstly, I would like to thank my main supervisor Associate Professor Stig Ollmar. My heartfelt thanks to you Stig, for all invaluable encouragement and advice in every aspect of this project. Without you believing in me and my work, I wouldn't have reached this far. Secondly I would like to thank my second supervisor Dr. Lars-Åke Brodin for all the expertise help and crucial suggestions; always with a smile and a new idea. I also would like to thank everyone at the Division of Medical Engineering for all the help and inspiration; my examiner Professor Håkan Elmkvist for pushing me ahead, tekn. lic. Camilla Carlsson, tekn. lic. Camilla Storaas, tekn. lic. Emil Söderkvist and Ph.D. student Peter Åberg – your work is inspiring and encouraging me,

Marita Kihlberg and Arja Grahn for guiding me through the administration work.

At St Jude Medical AB, I wish to thank the staff of the research group for all their help with the measurements and reviewing my work, especially Kjell Norén, Sven-Erik Hedberg, Jörgen Jagt and Jonas Andersson (Jörgen and Jonas no longer at St Jude Medical AB) and Nils Holmström. Thank you.

All my friends, Gabbe, Maria, Anna – for being there for me.

My grandmother Vera and my father Fred – I wish you could be here, I miss you.

My mother Gun for always being my mother and believing in me.

Monica, Ingegerd and Sandra for babysitting Mattias' and my son, Adam.

Adam, my wonderful, beautiful little sunshine in my life.

My beloved fiancée Mattias, for all your love and support, and for pushing me to finish my thesis.



# Contents

<b>ABSTRACT</b> .....	<b>III</b>
<b>PREFACE</b> .....	<b>IV</b>
<b>CONTENTS</b> .....	<b>VII</b>
<b>LIST OF PAPERS</b> .....	<b>IX</b>
<b>LIST OF FIGURES</b> .....	<b>X</b>
<b>ABBREVIATIONS</b> .....	<b>XII</b>
<b>1 INTRODUCTION</b> .....	<b>1</b>
1.1 THE HEART .....	1
1.2 DIASTOLE.....	4
1.3 ECHOCARDIOGRAPHY.....	5
1.4 IMPEDANCE .....	5
1.4.1 <i>Invasive intracardiac impedance</i> .....	9
1.4.2 <i>Intracardiac impedance configurations in pacemaker systems</i> .....	10
1.4.3 <i>Intracardiac impedance as sensor</i> .....	11
1.4.4 <i>Non-invasive transthoracic impedance</i> .....	12
1.5 THESIS OUTLINE .....	15
1.5.1 <i>Purpose and goals of the thesis</i> .....	15
<b>2 METHODS AND MATERIALS</b> .....	<b>17</b>
2.1 GENERAL.....	17
2.2 DATA COLLECTION.....	17
2.3 SIGNAL ANALYSIS .....	18
2.4 AC IMPEDANCE .....	19
2.5 PRE-CLINICAL STUDY, PAPER I.....	20
2.6 CLINICAL STUDY, PAPER II.....	21
<b>3 RESULTS</b> .....	<b>23</b>
3.1 GENERAL.....	23
3.2 PAPER I, PRE-CLINICAL STUDY .....	23
3.3 PAPER II, CLINICAL STUDY .....	27
3.4 SUMMARY OF RESULTS.....	29
<b>4 ETHICAL APPROVAL</b> .....	<b>31</b>
4.1 PAPER I, PRE-CLINICAL STUDY .....	31
4.2 PAPER II, CLINICAL STUDY .....	31
<b>5 DISCUSSION</b> .....	<b>33</b>
5.1 POLARIZATION .....	33
5.2 OBSERVATION OF THE NOTCH .....	33
5.3 THE NON-INVASIVE O-WAVE.....	34
5.4 NOTCH INTRACARDIAC EQUIVALENT OF TRANSTHORACIC O-WAVE.....	35
5.5 SUMMARY .....	37
<b>6 FUTURE WORK</b> .....	<b>39</b>
<b>7 CONCLUSIONS</b> .....	<b>41</b>
<b>REFERENCES</b> .....	<b>43</b>
<b>APPENDIX</b> .....	<b>47</b>



## List of Papers

---

This thesis is based on the following papers, which will be referred to using roman numerals I-II. All papers are included at the end of the thesis.

### Refereed papers

- I Karin Järverud, Stig Ollmar, Lars-Åke Brodin  
*Analysis of the O-wave in acute right ventricular apex impedance measurements with a standard pacing lead in animals*  
Medical and Biological Engineering and Computing (Med. & Biol. Eng. Comput.), 2002, **40(5)**, pp. 512-519
- II Karin Järverud, Börje Darpö, Lars-Åke Brodin, Stig Ollmar  
*Descriptive analysis and initial finding of O-wave in acute right ventricular apex impedance measured with a standard pacing lead in human (manuscript submitted)*

## List of Figures

Figure 1.1 A pacemaker system in a patient. ....	2
Figure 1.2 The anatomy of the heart. ....	3
Figure 1.3 The filling phases of the cardiac cycle as seen in schematically drawn curves of ventricular volume and pressure, together with ECG. In the ventricular pressure curves, the maximum (#) and minimum (£) slope of pressure is marked (maximum and minimum value of first derivative of pressure). These points in the heart cycle may serve as good indicators for opening and closing of valves respectively (see text). ....	4
Figure 1.4 Schematic picture of echocardiographical measurements of AV-plane valve blood flow pattern.(in this example, right ventricle is displayed in echocardiographical “window”).....	5
Figure 1.5 A current I is applied on the subject through two electrodes and the resulting voltage U is measured between another pair of electrodes in a so-called four-pole configuration .....	6
Figure 1.6 Ohm’s law.....	6
Figure 1.7 Measurement current is conducted through biomaterial in different way depending on frequency A; schematic picture of a cell with cell membrane and internal cell structure B; low frequency current is conducted through extracellular tissue space C; high frequency current is coupled capacitively through the cell membrane and into the internal cell structures (intracellular tissue) .....	8
Figure 1.8 ECG and impedance signal measured in sheep with a standard bipolar pacing lead in right ventricular apex. Measurement current: 10 $\mu$ A, 4kHz square wave.....	9
Figure 1.9 Electrode placement for non-invasive transthoracic impedance measurements (see text) .....	12
Figure 1.10 First derivative of transthoracic impedance, phonocardiography and apex cardiogram (schematically redrawn after LABABIDI et al., 1970 and PREWITT et al., 1975). ....	14
Figure 2.1 The methodology by which “averaged heart cycle signal” is calculated is described. In this example 8 heart cycles were identified to be analyzed, an ASCII file with these cycles were cut out from original WinDaq file and used in Matlab tool for further analysis. ....	18
Figure 2.2 Block diagram for the AC impedance box. ....	19
Figure 2.3 Impedance configuration in clinical study (paper II). The measurement current is applied between EP catheter electrodes 1 and 2. The resulting voltage is sensed between electrodes 1 and 2, or between 1 and 3 or between 1 and 4 (see text). ....	22
Figure 3.1 Example of intracardiac impedance signal (The top graph displays averaged intracardiac impedance (black curve) together with ECG, left	

- ventricular pressure (LVP) and right ventricular pressure (RVP). The bottom graph displays averaged heart cycle curve of first derivative of intracardiac impedance. (Heart cycle averaged signals using 18 sinus rhythm heartbeats in sheep. Average heart rate= $77.0 \pm 0.5$  bpm, average impedance= $607.5 \pm 52.0 \Omega$ .) ..... 24
- Figure 3.2 Echocardiographical measurements performed simultaneously with intracardiac impedance in sheep. The results from mitral blood flow and tricuspid AV-plane movement measurements are aligned for analysis purposes. An impedance notch is visually observed after rapid ventricular filling (E) but before ventricular filling caused by atrial contraction (A).. 25
- Figure 3.3 From the top: ECG, left ventricular pressure (LVP, black curve), right ventricular pressure (RVP, gray curve), first derivative of pressures and intracardiac impedance. Time difference is calculated as the time difference between the minima of first derivatives of pressures. For this particular animal, minimum of first derivative of RVP occurs 36 ms before minimum of first derivative of LVP. .... 26
- Figure 3.4 Example of intracardiac impedance signal in a healthy patient. The top graph displays averaged intracardiac impedance, the middle graph displays averaged heart cycle curve of first derivative of intracardiac impedance and the bottom graph is the normalized ECG. Heart cycle averaged signals using 18 sinus rhythm heartbeats in sheep. Average heart rate= $77.0 \pm 0.5$  bpm, average impedance= $607.5 \pm 52.0 \Omega$ .) ..... 27
- Figure 3.5 Definition of intracardiac diastolic notch: the first positive slope change in the negative diastolic impedance slope between end of T-wave and P-wave in the ECG. A slope change immediately at the end of T-wave is not considered to be an observed notch. .... 28
- Figure 5.1 The observation of notch is sometimes made more easily with the aid of standard deviation curve. .... 34

## Abbreviations

---

RV	Right Ventricle
LV	Left Ventricle
SV	Stroke Volume
EP study	Electro Physiological study
Z	Impedance
dZ/dt	First derivative of impedance

# 1 Introduction

---

## 1.1 The heart

In awake and resting humans, the heart beats approximately once every second. The heart rate is then said to be 60 beats per minute (bpm). Normally, the electrical activity of specialized cells in the sinus node is conducted throughout the cardiac conduction pathways inducing cardiac contractions in a frequent manner thus controlling the heart rate (HR, [bpm]). When the sinus node is controlling the heart rate, the heart is in a so-called sinus rhythm. When needed, the heart rate of a healthy heart can be increased dramatically through different physiological controlling mechanisms. The cardiac electrical activation pattern can be studied in the electrocardiogram, ECG, measured through electrodes placed on the subject's skin. The electrical activity can also be measured inside the heart with electrodes placed in the cardiac tissue (myocardium). The electrical activation pattern measured from inside the heart is called intracardiac electrogram, IEGM. Clinically the ECG is used for diagnostic purposes (such as myocardial infarction) and not the IEGM since the latter electrogram only registers the local electrical activity surrounding the intracardiac electrode.

If the cardiac conduction pathways are disrupted, the heart rate is often reduced (bradycardia) and the heart lacks ability to increase the pumping frequency and is therefore incapable to respond properly to physical demand. In addition, the heart rate in resting conditions is often too low. The

bradycardia patient is unable to live a normal life and needs a pacemaker system to maintain adequate heart rate (DAS and CARLBLOM, 1990). A pacemaker system consists of a pulse generator and one or two pacemaker leads and is normally implanted during local anesthesia. The tips of the leads are normally placed inside the heart as the leads are introduced through the venous blood vessels. The pulse generator is placed under the skin (subcutaneously).

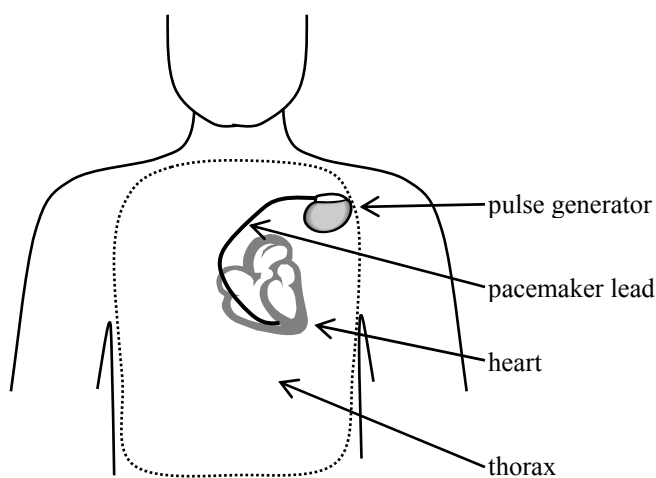
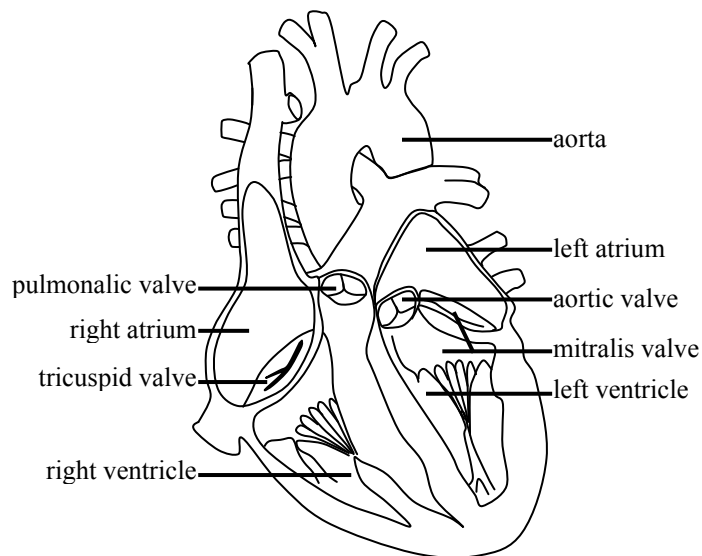


Figure 1.1 A pacemaker system in a patient.

The pacemaker system causes cardiac contraction as the pulse generator emits stimulation pulses to the cardiac tissue through the intravenous pacemaker leads. Modern pacemakers do not only maintain a basic heart rate by fixed rate stimulation. These systems are also designed to mimic the physiological heart rate behavior during physical load by controlling the stimulation rate with different types of sensors (ALT *et al.*, 1998; KARLÖF, 1974; LAU, 1992; NAPHOLZ *et al.*, 1987; 1990; SCHALDACH *et al.*, 1992;). So far, the over-all ambition has been to avoid sensors that would complicate the otherwise robust and standardized leads.

During every normal heartbeat, a volume of blood is ejected to all the organs of the body (stroke volume SV, [ml]). Normally this specific volume of blood is transported to the lungs (lesser or pulmonary circulation) and later

routed to the rest of the body (body or systemic circulation). When the blood is passed through the pulmonary circulation, the blood oxygen content is increased and blood carbon dioxide content is decreased through a gas exchange process in the lungs. The heart has four chambers (two atria and two ventricles) organized in two pumps. Right atrium and right ventricle is the pump for the pulmonary circulation whereas left atrium and left ventricle is the pump for the systemic circulation (RHOADES and TANNER, 1995). Four valves are positioned inside the heart making sure that blood flow is unidirectional.



*Figure 1.2 The anatomy of the heart.*

Since these two pumping units are connected one after the other (in series) it is important that each pump ejects the exact same amount of blood over a period of time. If not, an unbalanced distribution of blood volume between the pulmonary and systemic circulation will occur causing volume overload (edema).

## 1.2 Diastole

Every heartbeat has a filling phase (diastole) and an ejection phase (systole), Figure 1.3. During diastole, the heart muscle relaxes, mitral and tricuspid valves between the atria and the ventricles (situated in atrio-ventricular plane, AV-plane) open and the ventricles are passively filled with blood – rapidly at first in the rapid filling phase, and then slowly in the slow filling phase. When the slow filling phase has ended, the ventricles are filled with some additional blood as the atria contract.

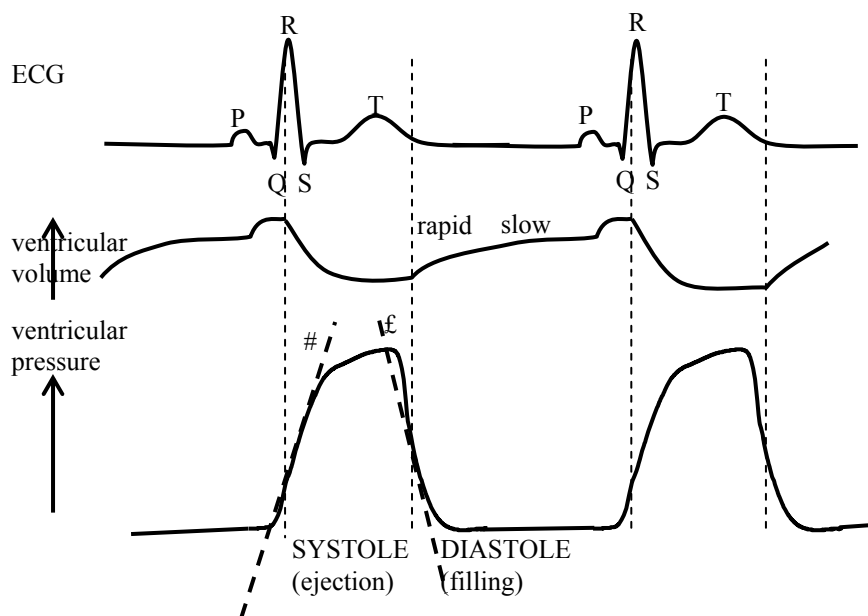


*Figure 1.3 The filling phases of the cardiac cycle as seen in schematically drawn curves of ventricular volume and pressure, together with ECG. In the ventricular pressure curves, the maximum (#) and minimum (£) slope of pressure is marked (maximum and minimum value of first derivative of pressure). These points in the heart cycle may serve as good indicators for opening and closing of valves respectively (see text).*

### 1.3 Echocardiography

A number of cardiac characteristics can be studied and evaluated by using echocardiography. In echocardiographical measurements, ultrasonic waves are transmitted to the subject (HATLE, 1986; 1987), and as the internal cardiac structures reflect these waves, live images of the working heart can be created and studied. Cardiac wall movements and blood flow patterns can be calculated and studied using the echocardiographical images. A common clinical way of determining filling characteristics in patients is to evaluate the blood flow pattern between atrium and ventricle in diastole, as seen in mitral and tricuspid valve blood flow, Figure 1.4.

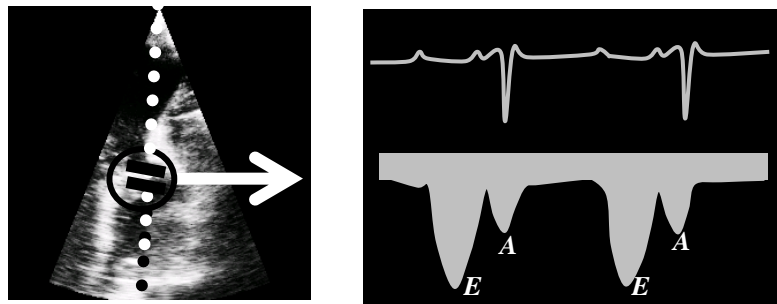


*Figure 1.4 Schematic picture of echocardiographical measurements of AV-plane valve blood flow pattern.(in this example, right ventricle is displayed in echocardiographical “window”)*

As described earlier, the filling phase can be divided into rapid or early filling and slow filling. Rapid early ventricular filling is displayed as a large peak E in mitral or tricuspid blood flow, and ventricular filling caused by atrial contraction is displayed as a smaller peak A.

### 1.4 Impedance

When a voltage source is connected to a conducting material, movement of free electrons of the material achieves an electrical current. As the voltage source has a positive and negative pole connected to the material in question, the free negatively charged electrons are attracted to the positive pole

and therefore tend to move in that direction. The properties of the achieved electrical current depend on the conducting characteristics of the material and also on the characteristics of the voltage signal. When the material is said to be purely resistive, the current level is independent on voltage frequency. The higher resistance ( $R$ , Ohm) the lower the resulting current ( $I$ , Amperes A) for a given voltage ( $U$ , Volt). This can be expressed in a reversed way; when a current source with current  $I$  (A) is applied to a conducting material with the resistance  $R$  (Ohm), a resulting voltage drop  $U$  (V) can be measured across the material, Figure 1.5.

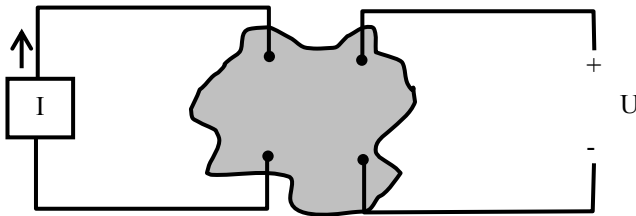


*Figure 1.5 A current  $I$  is applied on the subject through two electrodes and the resulting voltage  $U$  is measured between another pair of electrodes in a so-called four-pole configuration*

The voltage  $U$  can be calculated with the Ohm's law:

$$U=R*I$$

*Figure 1.6 Ohm's law*

However, if the material is composed of non-resistance components such as capacitors or inductors, the material is no longer resistive and frequency dependency is introduced. Ohm's law still applies, although resistance  $R$  is replaced with impedance  $Z$  (Ohm) in the formula. The impedance of a capacitor  $C$  is dependent on the frequency of the applied current or voltage source and the capacitor's capacitance,

$$\frac{1}{2\pi fC}$$

f, frequency (Hz); C capacitance (farad, F)

This means that the higher frequency, the lower impedance and vice versa.

Electrically, the cell membrane acts like a capacitor. In biological material the conduction is essentially ionic, i.e. the current is caused by movement of ions that are much bigger and heavier and have less mobility than electrons. If a measuring current of a very low frequency is applied over a biomaterial composed of many cells, the current is mainly conducted through the fluid surrounding the cells because it is blocked to pass through the cell membrane. On the other hand, if a high frequency measuring current is applied it would conduct through the cell membrane to the interior of the cell and thus revealing the electrical properties of the internal cell structures.

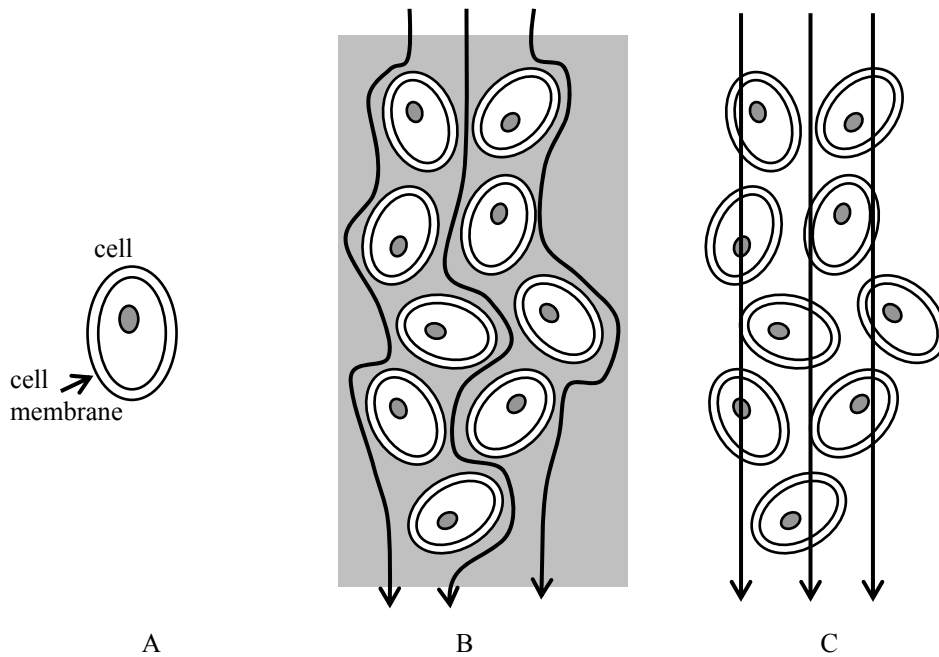


*Figure 1.7 Measurement current is conducted through biomaterial in different way depending on frequency*  
*A; schematic picture of a cell with cell membrane and internal cell structure*  
*B; low frequency current is conducted through extracellular tissue space*  
*C; high frequency current is coupled capacitively through the cell membrane and into the internal cell structures (intracellular tissue)*

By applying measurement current and changing the current frequency over a wide range, and registering the voltage response, electrical bioimpedance can be measured and different layers, components or organs of the biomaterial can be studied. (FOSTER and SCHWAN, 1989, GABRIEL *et al.*, 1996, ZHAO, 1993). In fact, different changes in for instance human skin can be detected much earlier compared to conventional methods by using electrical impedance (NICANDER, 1998). In electrical impedance tomography (EIT), internal organs can be imaged (BOONE *et al.*, 1997). In general, the impedance of cardiac tissue is higher compared to the impedance of blood, i.e. electrical current is more easily conducted through blood. In other words, the conductivity of blood is higher compared to the conductivity of cardiac tissue.

In invasive impedance the measurement is performed using the electrodes placed inside the subject (see 1.4.1 on page 9). By applying

measuring current and sensing resulting voltage from electrodes positioned on the subject's skin, non-invasive impedance is obtained (see 1.4.4 on page 12).

### 1.4.1 Invasive intracardiac impedance

Invasive impedance in general is measured from inside the body. Intracardiac impedance measurements are performed locally inside the heart and are therefore invasive. Intracardiac impedance measured through pacemaker leads reflects ventricular volume and can be used as a sensor signal, see Figure 1.8.

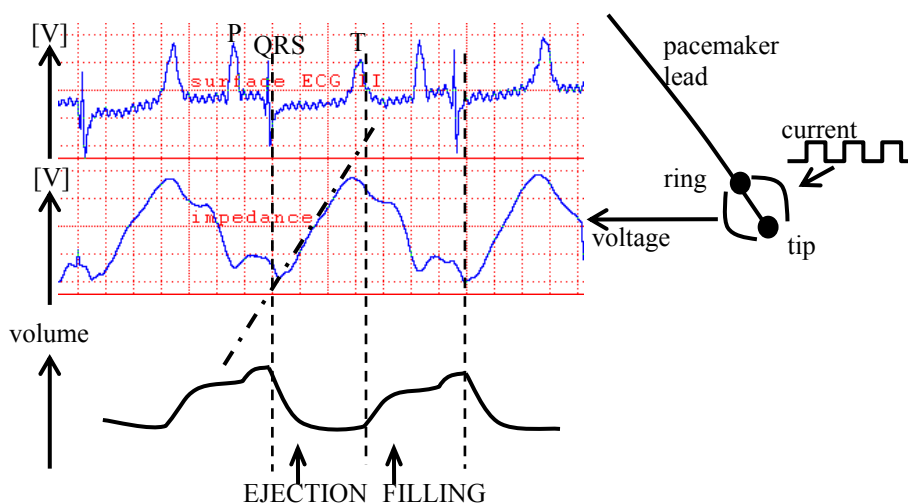


Figure 1.8 ECG and impedance signal measured in sheep with a standard bipolar pacing lead in right ventricular apex. Measurement current:  $10\mu\text{A}$ , 4kHz square wave.

The intracardiac impedance signal in Figure 1.8, is in this example presented as the voltage between tip and ring of a standard bipolar pacing lead in right ventricular apex (a square-wave measuring current is connected to the same pair of electrodes). During systole, the intracardiac impedance increases rapidly as a result of the ejection of blood. The impedance slope in this interval can represent the level of contraction force, contractility (see tilted dotted line in impedance signal in figure above). At end-systole, when blood has been ejected, the lead tip is surrounded by myocardial tissue, although there is a residual volume of blood remaining in the ventricles. The relatively high

impedance of the myocardium is dominating the resulting impedance at this point, thus causing the maximum impedance in the intracardiac impedance curve. As the ventricles are filled with blood in diastole, the impedance is decreased. Maximum ventricular volume is present after atrial contraction. At this point, in end-diastole just prior to ventricular contraction, the intracardiac impedance is at its lowest point, since the measuring electrodes are surrounded with blood with higher conductivity. At this point intracardiac impedance has reached a low value corresponding to ventricular end-diastolic volume.

#### 1.4.2 Intracardiac impedance configurations in pacemaker systems

With a pacemaker system consisting of a standard bipolar pacemaker lead in right ventricle and a subcutaneously placed pulse generator, there are three electrodes at hand for impedance measurements. The measurement current and measurement voltage can be applied in 9 different ways:

	Measurement current	Measurement voltage
1.	tip-ring	tip-ring
2.	tip-ring	tip-indifferent
3.	tip-ring	ring-indifferent
4.	tip-indifferent	tip-ring
5.	tip-indifferent	tip-indifferent
6.	tip-indifferent	ring-indifferent
7.	ring-indifferent	tip-ring
8.	ring-indifferent	tip-indifferent
9.	ring-indifferent	ring-indifferent

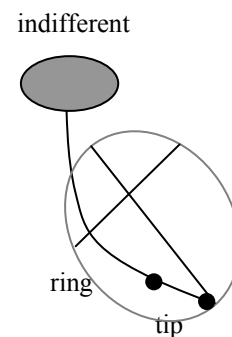


Table 1. In an implantable pacemaker system with one bipolar pacemaker lead and pulse generator capsule, 9 different impedance configurations are available.

In this thesis, the only configuration that has been studied is the first configuration; i.e. measuring current applied between tip and ring of a standard bipolar pacemaker lead in right ventricular apex and the sensing voltage between the same pair of electrodes.

The measured voltage is modulated both by cardiac events and by thoracic movements caused by respiration. Applying the measuring current

and/or sensing the voltage over the thoracic cavity (e.g. the indifferent electrode is used) will increase the level of respiratory modulation of the resulting impedance signal. On the other hand, by performing the impedance measurements between the tip and ring, the impedance is mainly reflecting cardiac activity.

### 1.4.3 Intracardiac impedance as sensor

As previously mentioned, modern pacemaker systems are designed to maintain the heart rate in a physiological way by measuring physiological parameters for stimulation control. A pacemaker system does not require any specialized leads or sensors to measure intracardiac impedance. The intracardiac impedance is generated and processed by pulse generator electronics using the available pacemaker lead electrodes and pulse generator capsule. Because of this important advantage, and the need for physiological stimulation control, all major pacemaker manufacturers have pacemaker models using impedance in some way: respiration controlled pacemaker (ALT *et al.*, 1998; NAPHOLZ *et al.*, 1987; 1990) and contractility controlled pacemaker (SCHALDACH *et al.*, 1992).

Some applications measure stroke volume using left ventricular conductance measured with the multi-electrode “Baan” catheter temporarily positioned in left ventricle (BAAN *et al.*, 1984). This technique has also been studied in the right ventricle (STAMATO *et al.*, 1995). The conductance catheter technique requires calibration steps where the conductance of blood is measured and also where the “parallel conductance” is registered. The parallel conductance is a correction term caused by the structures surrounding the ventricular cavity. The calibration steps are necessary in order to get absolute values of ventricular volume. Since these calibration steps are not possible in implantable devices, only relative measurements of volume are possible in pacemaker systems. Although studies using stroke volume for stimulation rate control have been performed (SALO *et al.*, 1984; CHIRIFE, 1991; CHIRIFE *et al.*, 1993) no such pacemaker systems are commercially available at the present

time. Absolute values of volume may be very difficult to measure, if at all possible, although some non-invasive instruments are available on the market.

#### 1.4.4 Non-invasive transthoracic impedance

Non-invasive transthoracic impedance measurement systems are developed and described by others (KUBICEK *et al.*, 1966; 1974). In this setup, four band electrodes are placed around the neck and abdomen of the subject, Figure 1. The measuring current is connected to the outer band electrodes and the resulting voltage is sensed from the two inner band electrodes. With this system non-invasive transthoracic impedance is registered.

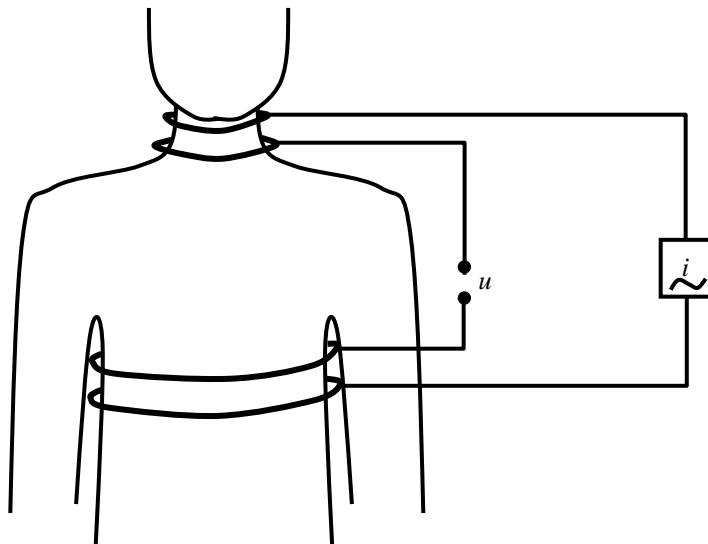


Figure 1.9 Electrode placement for non-invasive transthoracic impedance measurements (see text)

Numerous studies have analyzed how the transthoracic impedance can be used to measure stroke volume and cardiac output (CO, stroke volume  $\times$  heart rate, [l/min]) (KUBICEK *et al.*, 1966; 1974, MUZI *et al.*, 1985, DONOVAN *et al.*, 1986). The time relation between transthoracic impedance, ECG and cardiac time intervals is mainly studied using the first derivative of the transthoracic impedance cardiogram,  $dZ/dt$  (LABABIDI, 1978, KUBICEK *et al.*, 1974; KARNEGIS and KUBICEK, 1970). Lababidi *et al.* did a thorough definition of all curve segments in the first derivative of non-invasive transthoracic impedance cardiogram ( $dZ/dt$ ) and its relation to phonocardiography

(LABABIDI *et al.*, 1970). In fact, most of the impedance cardiogram work refers to this particular document for interpretation of transthoracic impedance curve segments. (In phonocardiography, sounds of valve closure “snaps” and blood flow pattern are registered and studied.) Studies have shown that the  $dZ/dt$  can be used to measure a number of important hemodynamic properties. In the diastolic  $dZ/dt$  there is a so called O-wave coinciding with mitral valve opening seen in apex cardiogram (LABABIDI, 1978; RAMOS, 1977), Figure 1.10. Apex cardiogram is the pressure pulsation caused by cardiac contractions in the apex area measured on the subject’s chest.

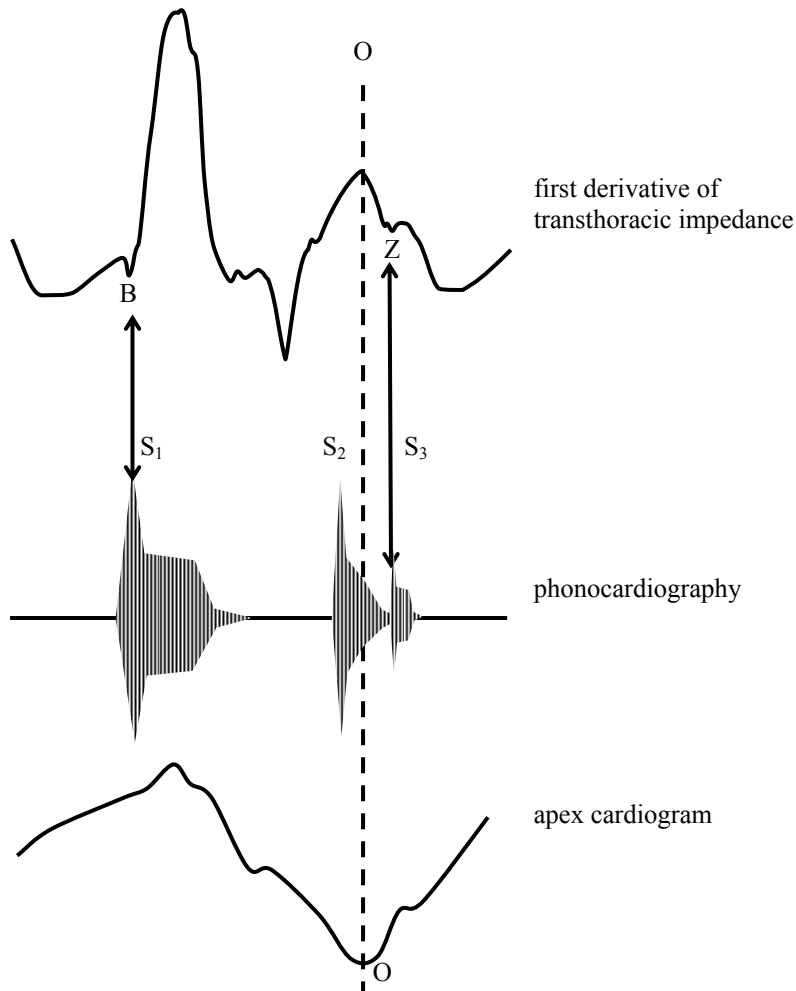


Figure 1.10 First derivative of transthoracic impedance, phonocardiography and apex cardiogram (schematically redrawn after LABABIDI *et al.*, 1970 and PREWITT *et al.*, 1975).

The transthoracic impedance O-wave is more dominating in patients with impaired cardiac function and is increased in size in patients with mitral valve leakage (regurgitation), volume overload and increased left atrial pressure. (SHOEMAKER *et al.*, 1994; KARNEGIS *et al.*, 1981; HUBBARD *et al.*, 1986; WOLTJER *et al.*, 1997; ALT *et al.*, 1998; PICKET and BUELL, 1993; MUZI *et al.*, 1985).

The transthoracic impedance is interpreted to contain impedance data originating from the heart. However, studies have showed that the so called

cardiac signal in the non-invasive impedance signal also can be retrieved from measurements performed on for example an arm (KAUPPINEN, 1999). The reason for this is that pulsations caused by cardiac contractions are transmitted to the body tissue of the arm. Therefore, the true explanation for cardiac signal in transthoracic impedance, and therefore also the O-wave, is complex and not straightforward.

## **1.5 Thesis outline**

In intracardiac impedance measurements performed in research projects at St Jude Medical AB, a small slope change in the diastolic phase was visually observed. These initial findings were made in measurements in animal subjects (pre-clinical measurements) and are analyzed and reported in paper I. In order to see if this slope change (notch) also can be observed in measurements in humans (clinical measurements), intracardiac measurements made in a human study were analyzed and reported in paper II.

### **1.5.1 Purpose and goals of the thesis**

The purpose and goals of this thesis are in general to describe and analyze diastolic intracardiac impedance, and specifically to describe, analyze and explain a specific diastolic intracardiac impedance waveform called notch.

One hypothesis for the notch is that it may be caused by a ventricular wall movement generated by the change from rapid blood inflow to slow blood inflow associated with diastole going from rapid filling to slow filling. This Ph.D. work is aimed to explain the mechanisms behind this impedance behavior.

The purpose of the present thesis was also to find out if the intracardiac impedance contains a similar O-wave as in the non-invasive impedance, which would strongly suggest that non-invasive O-wave originates from the heart.



## 2 Methods and materials

---

### 2.1 General

This thesis is based on two studies described below (paper I and paper II). All impedance measurements have been performed with the same impedance equipment described below. The basic principle for data collection is the same in both studies. The signal analysis in these two studies have been performed using the same methodology.

### 2.2 Data collection

In both studies, several signals were recorded digitally on DAT tapes (RD-145T 16 channel DAT tape recorder, DC-5 kHz, anti-aliasing filter, TEAC America, Inc.). The anti-aliasing filter is used to prevent the registered data to be disturbed by signals containing frequencies above 5 kHz. In paper I, the data was also simultaneously stored on computer hard disk at the time of the test (250 Hz or 500 Hz sampling frequency, special binary file format, WINDAQ software, DATAQ Instruments, Inc.). In paper II, the data on DAT tapes were transferred to WINDAQ binary files at a later point, with a sampling frequency of 1 kHz.

## 2.3 Signal analysis

Typically 10-30 heart cycles of sinus rhythm signals of specific time segments were transferred to PC calculating program called MATLAB (The MathWorks, Inc.) for calculation of “averaged heart cycle appearance”. This was done to study typical signal appearance of one heart cycle, Figure 2.1.

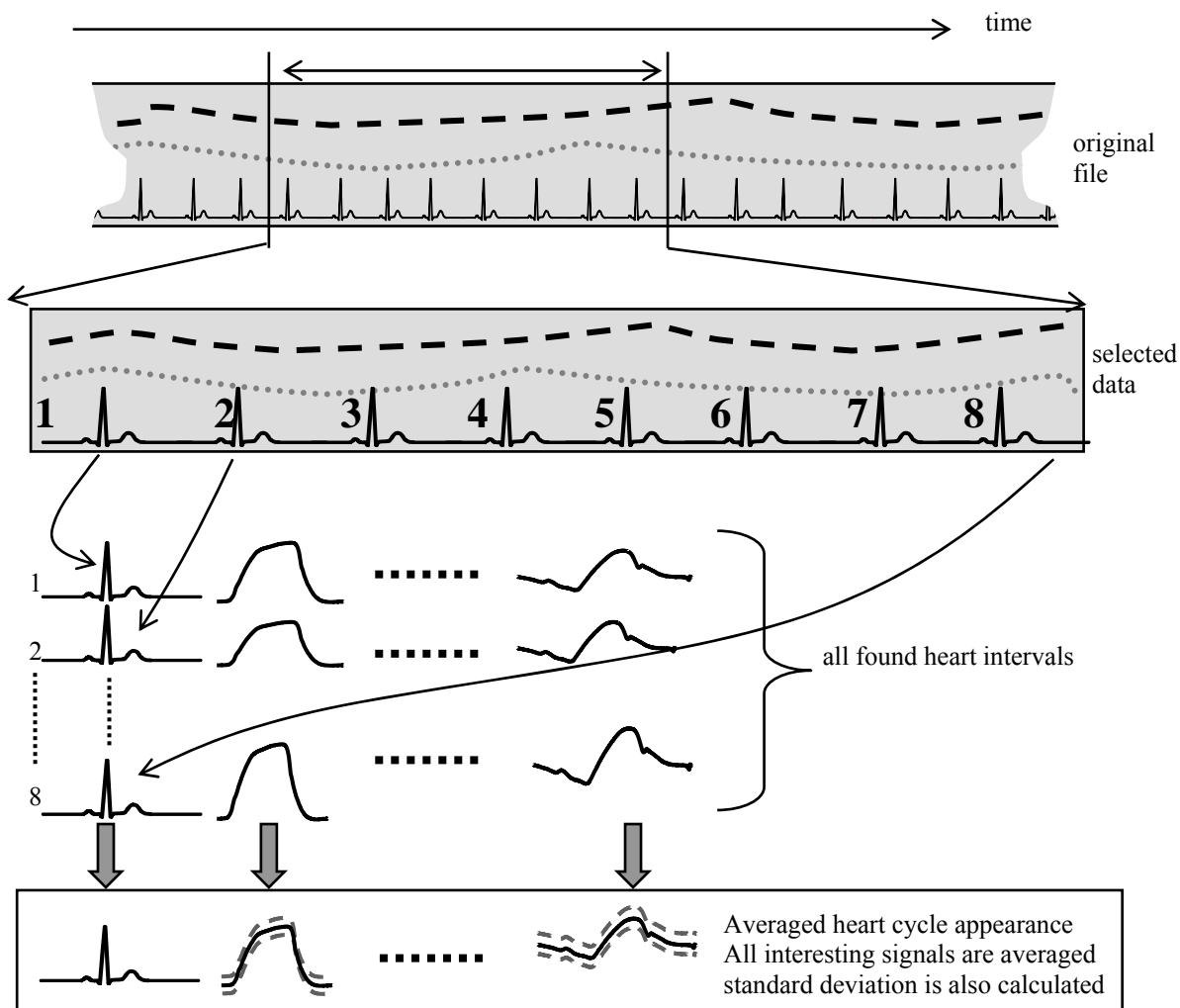


Figure 2.1 The methodology by which “averaged heart cycle signal” is calculated is described. In this example 8 heart cycles were identified to be analyzed, an ASCII file with these cycles were cut out from original WinDaq file and used in Matlab tool for further analysis.

In the selected data of signals, all ECG R-waves were detected and thus all available heart intervals were identified. For each sample in the ensemble of signal data, both average and standard deviation value were calculated, thus

forming an averaged curve form (KELSEY and GUETHLEIN, 1990; MUZI *et al.*, 1985) together with standard deviation curve form over one heart cycle. First derivative of impedance was calculated in MATLAB using the “gradient” function. This derivative impedance signal was then low pass filtered with a cut off frequency of 50 Hz in paper I and 35 Hz in paper II (4<sup>th</sup> order Butterworth low-pass filter, zero-phase filtering), forming the derivative signal presented here.

## 2.4 AC impedance

All impedance measurements performed in this thesis have been performed using the same impedance equipment described below.

The AC-impedance equipment is designed and built at St Jude Medical AB. The right ventricular impedance signal in the present thesis was measured as the voltage difference between tip and ring on the lead positioned in the right ventricular apex, with measurement current applied between the same electrodes Figure 2.2.

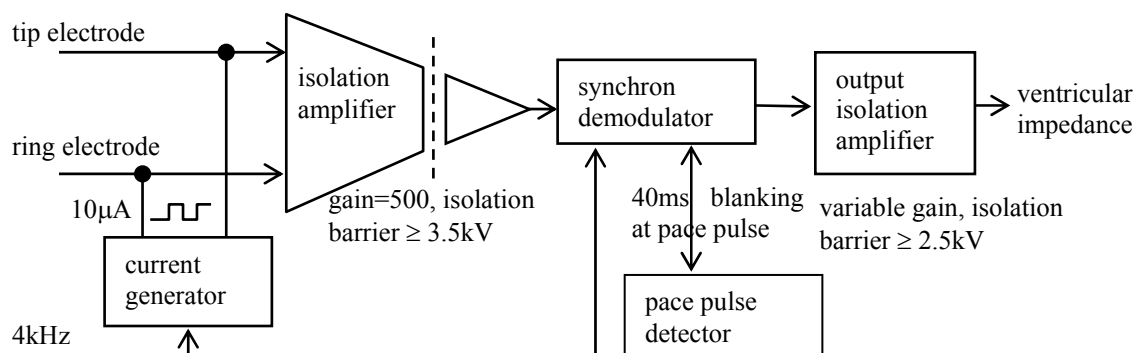


Figure 2.2 Block diagram for the AC impedance box.

The current generator generates a 4 kHz square wave measurement current. The choice of frequency was made due to the fact that pacemakers at that time of design had a 32 kHz crystal frequency and telemetry at 4 kHz, and the circuitry design was aimed to fit the reality of pacemaker technology. The

blood impedance is also mainly resistive at this frequency (GABRIEL *et al.*, 1996; FOSTER and SCHWAN, 1989) and higher frequencies would drain pacemaker battery too much.

The voltage response signal is amplified 500 times in an isolation amplifier with isolation barrier of at least 3.5 kV. The synchronous demodulator samples every half wave of the square wave response signal and negative samples are inverted. All samples are added up resulting in an impedance signal with a band width of 0-180 Hz. The output isolation amplifier (isolation barrier 2.5 kV) adjusts the output level to establish a volt-to-ohm relation. The demodulator is also connected to a pace pulse detector that considers a sensed impedance level above 900 ohms as a detected stimulation pulse. When a stimulation pulse is detected the pace pulse detector returns a blank signal to the demodulator that turns the demodulation off for 40 ms. This minimizes disturbances from the stimulation pulse on the impedance signal.

## 2.5 Pre-clinical study, Paper I

Impedance data from 9 animals over a period of 2 years (1996-1997) were analyzed. The procedure in anesthesia, pacemaker lead type, protocol and impedance measurement equipment were similar in all experiments. All catheters and leads were implanted transvenously. The pacemaker lead type used was a standard bipolar, MEMBRANE 1401T, Pacesetter, Inc. In order to ensure anesthesia stability, manual notes of heart rate, blood pressure, blood temperature and blood gas sample results were made continuously throughout each test. As discussed in paper I, transesophageal echocardiography measurements were performed together with similar signals as described above in an additional animal subject. (In transesophageal echocardiography, the probe is positioned inside esophagus producing a much clearer image compared to regular echocardiography with the probe positioned on the

subject's chest.) The procedure in anesthesia, protocol and pacemaker lead type was similar to the other 9 tests.

## 2.6 Clinical study, Paper II

Intracardiac impedance data was measured in 20 patients during the observational period following a catheter ablation in an electrophysiological procedure (EP). In an EP procedure, awake patients with unnormal cardiac conduction pathways (that may cause heart palpitations with a too high heart rate) are examined during local anesthesia. The pathological pathways are localized by temporarily positioning several intracardiac multielectrodes in the cardiac tissue region of interest. The small area in the cardiac tissue that causes the arrhythmia is then destroyed (ablated) by high frequency current causing a high temperature locally. After ablation, there is an observational period where the patient is normally in sinus rhythm, after which the ablation success is verified. All patients enrolled for this study had sinus rhythm during the impedance measurements. All measurements were performed with a standard four-polar EP catheter (standard quadripolar EP-catheter USCI, C.R. Bard Inc., New Jersey, USA). The 20 patients were divided into two groups. In one group of 10 patients the impedance was measured at rest during five minutes from three different pairs of electrodes: a) electrodes 1 (distal, in apex) and 2 (10 mm inter-electrode distance), b) electrodes 1 and 3 (20 mm) and c) electrodes 1 and 4 (30 mm), Figure 2.3

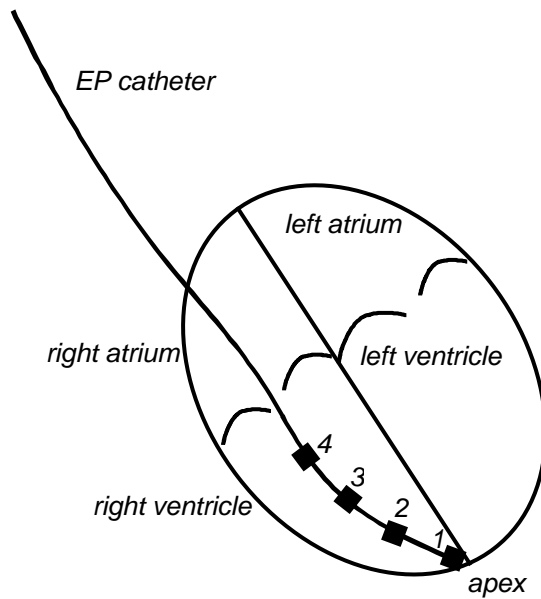


*Figure 2.3 Impedance configuration in clinical study (paper II). The measurement current is applied between EP catheter electrodes 1 and 2. The resulting voltage is sensed between electrodes 1 and 2, or between 1 and 3 or between 1 and 4 (see text).*

In the second group of 10 patients, the impedance was measured between two different pairs of electrodes at rest and was thereafter repeated during drug induced increase of cardiac workload. The measurements were performed between electrodes 1 and 2 (10 mm inter-electrode distance) and 1 and 3 (20 mm). An increase in the cardiac workload was achieved with an infusion of isoproterenol (2  $\mu\text{mol/ml}$ ) which was titrated to obtain a heart rate of 110-120 bpm. Measurements were started when a stable heart rate had been established.

## 3 Results

---

### 3.1 General

All impedance measurements reported in paper I and paper II were made during sinus rhythm.

### 3.2 Paper I, pre-clinical study

Intracardiac impedance signals from 9 animals (7 sheep and 2 dogs) under general anesthesia were analyzed.

The impedance signal shape varies remarkably from one individual to another, although the main shape with the lowest point close to R-wave in ECG and highest point close to end of T-wave still remains (with one exception described in detail in Paper I). The averaged impedance curve form in sheep is displayed in Figure 3.1.

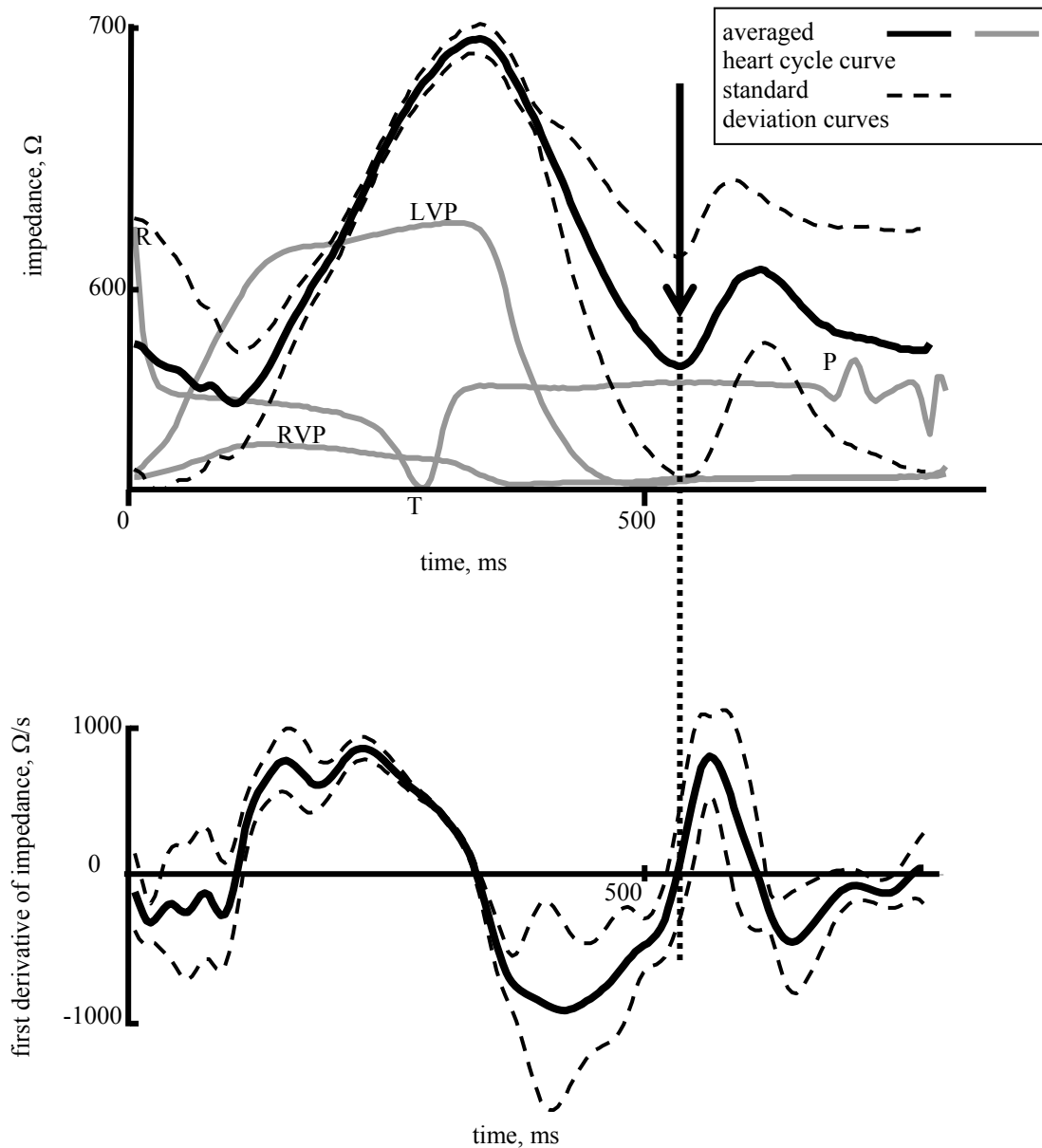
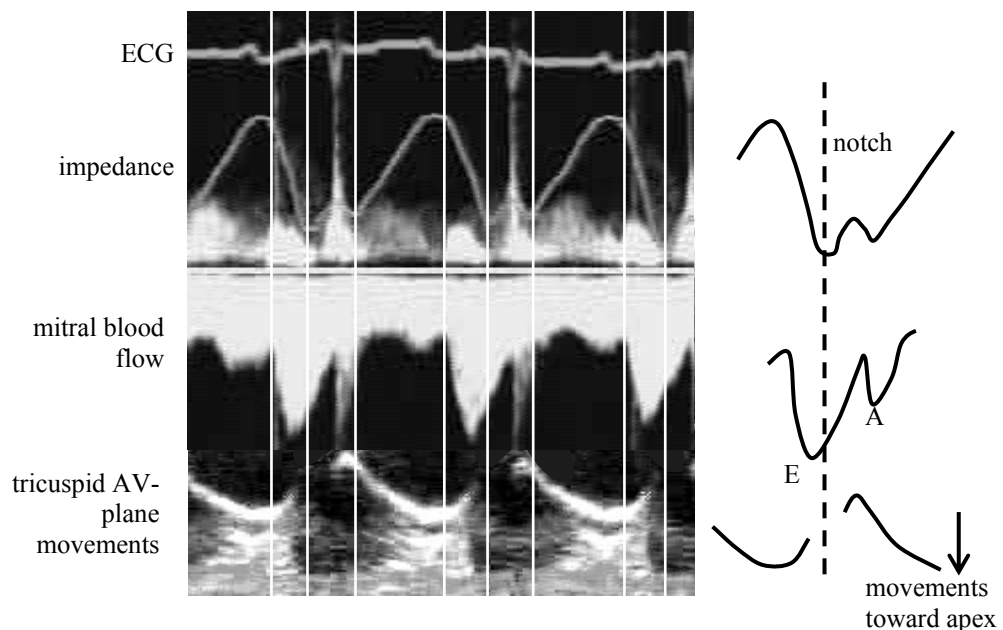


Figure 3.1 Example of intracardiac impedance signal (The top graph displays averaged intracardiac impedance (black curve) together with ECG, left ventricular pressure (LVP) and right ventricular pressure (RVP). The bottom graph displays averaged heart cycle curve of first derivative of intracardiac impedance. (Heart cycle averaged signals using 18 sinus rhythm heartbeats in sheep. Average heart rate= $77.0 \pm 0.5$  bpm, average impedance= $607.5 \pm 52.0 \Omega$ .)

In 8 of first 9 animal subjects (89%), a visible and consistent impedance slope change (notch) was visually observed in the early cardiac filling phase (Figure 3.1). The notch position is taken as the point at which the impedance

slope changes in the diastolic phase. In the first derivative of intracardiac impedance the notch can be detected as the first zero-crossing after maximum in the original impedance. In the additional measurement (10<sup>th</sup> animal) with simultaneous echocardiographical measurements of mitral blood flow, a notch was visually observed similar to the other experiments. As displayed in Figure 3.2 it occurs shortly after rapid filling as seen as E-wave, but prior to (left) ventricular filling caused by (left) atrial contraction (A-wave).



*Figure 3.2 Echocardiographical measurements performed simultaneously with intracardiac impedance in sheep. The results from mitral blood flow and tricuspid AV-plane movement measurements are aligned for analysis purposes. An impedance notch is visually observed after rapid ventricular filling (E) but before ventricular filling caused by atrial contraction (A).*

As the intracardiac impedance is measured on the right side, tricuspid valve operation may have some influence on notch and was therefore investigated further in the 10<sup>th</sup> animal. In Figure 3.2, the movements of the tricuspid AV-plane is somewhat unclear at the time of the notch. As described earlier, a good marker for detection of tricuspid and mitral valve opening is the minimum of first derivative of right and left ventricular pressure respectively. In order to further indicate when the tricuspid and mitral valves open, first derivative for right and left ventricular pressures were calculated and minimum peaks of these signals were detected for each heart cycle in all 10 animals.

These peaks can be viewed as time points where tricuspid valve and mitral valve open, see Figure 3.3 (same animal as in Figure 3.1). For each heart cycle, the time difference between these two peaks was calculated, estimating the time difference between opening of tricuspid and mitral valve.

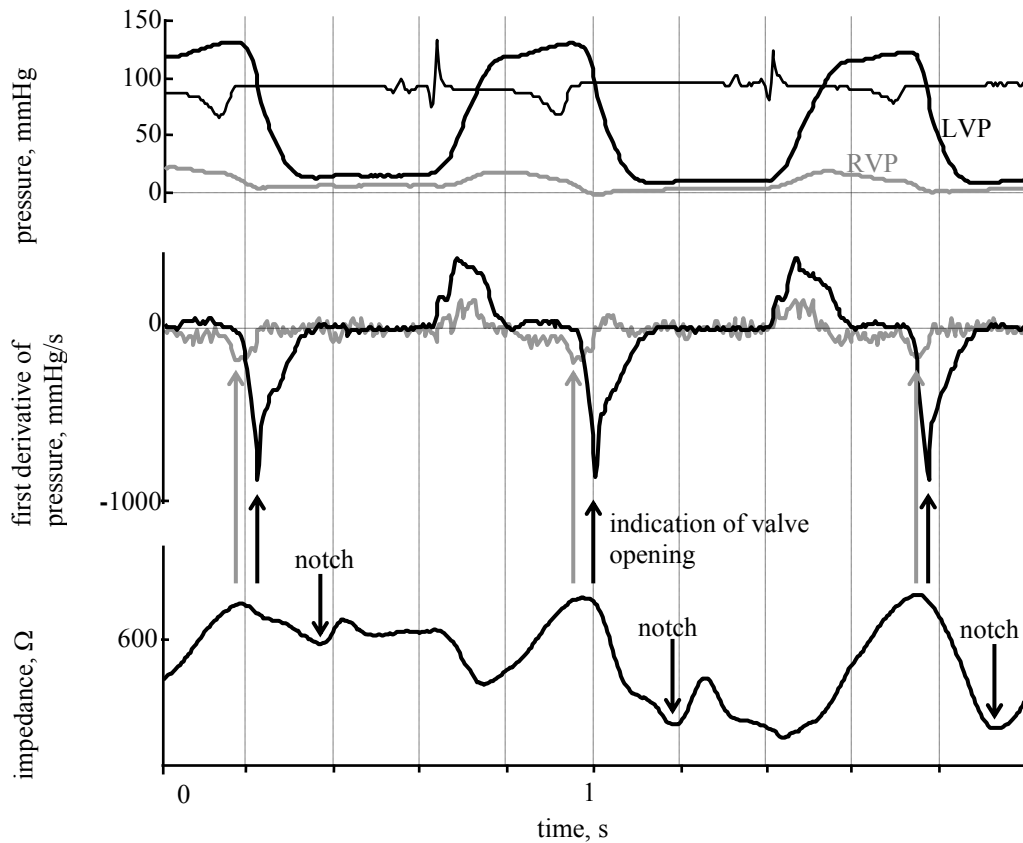


Figure 3.3 From the top: ECG, left ventricular pressure (LVP, black curve), right ventricular pressure (RVP, gray curve), first derivative of pressures and intracardiac impedance. Time difference is calculated as the time difference between the minima of first derivatives of pressures. For this particular animal, minimum of first derivative of RVP occurs 36 ms before minimum of first derivative of LVP.

In one animal, no data of left ventricular pressure were available. In 7 of the remaining 9 animals, the minimum of first derivative of right ventricular pressure occurred 23.6 ms (standard deviation 24.4 ms) before minimum of first derivative of left ventricular pressure. This result suggests that tricuspid valve opens 23.6 ms before mitral valve.

### 3.3 Paper II, clinical study

With two exceptions, mean impedance was increased during drug induced work load in the second group. The impedance signal shape varied remarkably from one individual to another, although the main shape with the lowest point close to R-wave in the ECG and highest point close to end of T-wave still remained. In Figure 3.4, an example of right ventricular impedance in a healthy patient with normal cardiac function at rest condition is displayed.

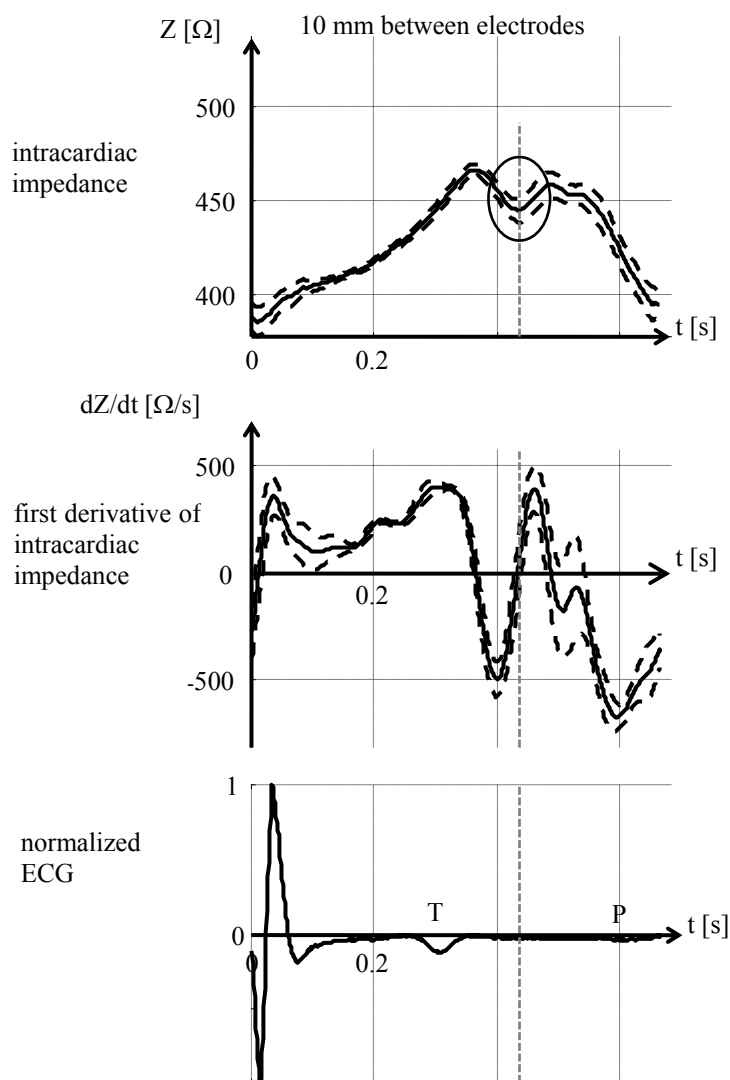


Figure 3.4 Example of intracardiac impedance signal in a healthy patient. The top graph displays averaged intracardiac impedance, the middle graph displays averaged heart cycle curve of first derivative of intracardiac impedance and the bottom graph is the normalized ECG. Heart cycle averaged signals using 18 sinus rhythm heartbeats in sheep. Average heart rate= $77.0 \pm 0.5$  bpm, average impedance= $607.5 \pm 52.0 \Omega$ )

The notch is defined as the first positive slope change in the negative diastolic impedance slope between end of T-wave and P-wave in the ECG, Figure 3.5.

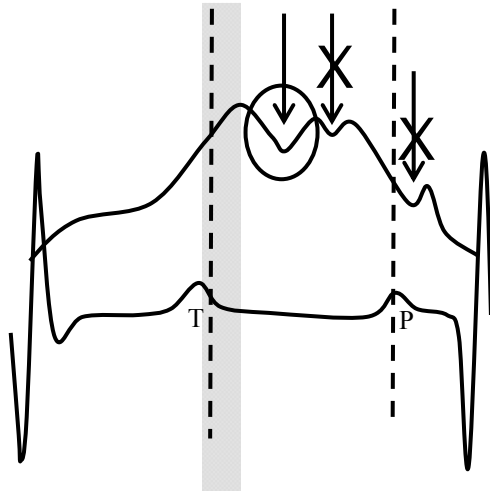


Figure 3.5 Definition of intracardiac diastolic notch: the first positive slope change in the negative diastolic impedance slope between end of T-wave and P-wave in the ECG. A slope change immediately at the end of T-wave is not considered to be an observed notch.

In 80% or more of the patients (depending of the inter-electrode distance and group), the notch was observed in early cardiac filling phase (see ring mark in Figure 3.4). In Table 2 below, the notch occurrence is presented in more detail.

Number of patients and impedance configurations in each	visible notch in
10 mm distance tip-ring (20 patients)	90% (18 of 20 patients)
20 mm distance tip-ring (20 patients)	100% (20 of 20 patients)
30 mm distance tip-ring (10 patients)	90% (9 of 10 patients)
10 mm distance tip-ring, isoproterenol (10 patients)	80% (8 of 10 patients)
20 mm distance tip-ring, isoproterenol (10 patients)	80% (8 of 10 patients)

Table 2. Notch occurrence in paper II. Depending on tip-ring distance and group, the notch occurrence varies between 80-100 %.

In order to investigate how the notch was affected by heart rate, the time between the R-wave in the ECG and the notch is plotted versus heart rate. The R-to-notch time is normalized with regards to average heart cycle interval. As shown in paper II, the R-notch time varies exponentially with heart rate ( $r^2=0.95$ ).

### 3.4 Summary of results

The signal analysis creating averaged curve forms and standard deviation curve forms present the data conveniently. In both studies, a slope change in diastolic intracardiac impedance was visually and consistently observed. The slope change, notch, is seen in 9 of 10 animals (90%) in paper I and in over 80% of the patients in paper II. In some cases the notch produced a large bump in diastolic impedance, whereas in other cases the notch only produced a small change in intracardiac impedance slope. In one animal subject (paper I), echocardiographical measurements of mitral blood flow performed simultaneously with intracardiac impedance measurements showed that the notch occurred after rapid ventricular filling E but before ventricular filling caused by atrial contraction A. In the human data in paper II, the R-notch time varies exponentially with heart rate ( $r^2=0.95$ ).



## **4 Ethical approval**

---

The ethic approvals are found in the appendix.

### **4.1 Paper I, pre-clinical study**

The local Ethics Committee has approved the animal measurements. All animals received human care in compliance with the European Convention on Animal Care.

### **4.2 Paper II, clinical study**

The Hospital's Human Ethics Committee approved the research protocol and all patients gave written informed consent prior to the test.



## 5 Discussion

---

### 5.1 Polarization

If the current injecting electrodes and voltage sensing electrodes are separated in a 4-electrode configuration the detection of polarization would be avoided (such as in method described in transthoracic impedance measurements, Figure 1. However, in the 2-electrode measurement setup used in this thesis, there was no net charge to the test subject since the current used was truly bi-phasic. Therefore, the signal did not itself cause polarization. Also, the self polarization, i.e. the composition of different bio-materials and electrode materials in the electrochemical environment, is a slow process and such alteration of the total impedance should not cause any contribution in our frequency range of measurements. The electrode/tissue interface as such, must therefore be regarded as fairly stable and will not change the shape of the impedance pattern in the time scale important for this work.

### 5.2 Observation of the notch

The intracardiac impedance slope change is visually observed, using the averaged curve forms calculated as described in 2.3 on page 18. Of course, a computerized and automatic detection of notch is preferable but as the explanation and description of the notch has been prioritized in this thesis, no such detection algorithm has yet been developed.

The observation of notch is sometimes made more easily by using the standard deviation curve as described in Figure 5.1 below.

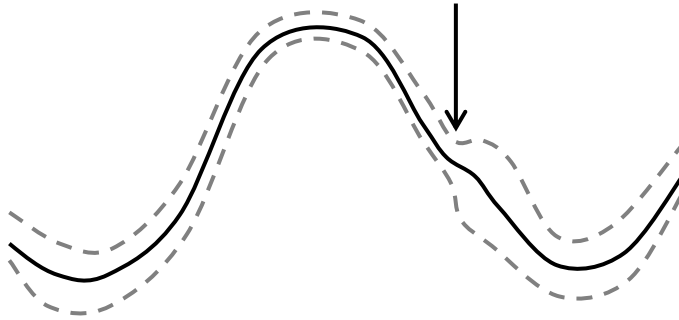


Figure 5.1 The observation of notch is sometimes made more easily with the aid of standard deviation curve.

### 5.3 The non-invasive O-wave

Lababidi et al. did a thorough definition of all curve segments in the first derivative of non-invasive transthoracic impedance ( $dZ/dt$ ) and its relation to phonocardiography (LABABIDI *et al.*, 1970). In fact, most of the impedance cardiogram work refers to this particular document for interpretation of transthoracic impedance curve segments, Figure 1.10. Although KARNEGIS and KUBICEK, 1970, denotes this inflection in transthoracic diastolic impedance as the V-wave (and as  $V'$  in the first derivative of transthoracic impedance) O-wave is the overall dominating name. It seems that the transthoracic O-wave got its name from O-wave curve segment of the apex cardiogram, merely because they coincide in the heart cycle. It also seems that the fact that impedance O-wave coincide with mitral valve opening snap does not raise any doubtful questions as to whether the O-wave really is caused by mitral valve movements or not. In fact, the origin of the cardiac portion of transthoracic impedance (and therefore also the O-wave) is truly complex and not straight forward (KAUPPINEN, 1999). It is therefore not proven without doubt that transthoracic O-wave really is caused by intracardiac events. A clear explanation of origin of the O-wave in transthoracic impedance has been discussed by others (LABABIDI, 1978; RAMOS, 1977) but is yet to be found.

Prewitt et al. claim that the O-wave in apex cardiogram is not related to mitral valve movement. This work claim that it correlates more closely with the peak rate of outward wall movement in early rapid filling (PREWITT *et al.*, 1975). Their work does not involve impedance measurements at all, but is well worth mentioning here since it provides interesting theories on the true reason for the O-wave in the apex cardiogram, and therefore also for the transthoracic impedance O-wave.

In 91 patients studied by Lababidi et al., 85.5 % displayed a visible O-wave. In work by Mattar et al. 86% in 913 impedance tracings measured in 100 patients displayed a visible O-wave (MATTAR *et al.*, 1991). Lababidi et al. particularly studied the O-wave in transthoracic  $dZ/dt$  signal simultaneously with the apex cardiogram in 10 patients with mitral stenosis. In 6 of these specific patients, the impedance O-wave was exactly simultaneous with the opening of mitral valve, seen as the “maximal vibration of the phonocardiographic opening snap”. In the remaining 4 patients, the impedance O-wave was found within 10 ms.

#### **5.4 Notch intracardiac equivalent of transthoracic O-wave**

One immediate and incorrect conclusion as to how the notch occurs is to say that it is simply the “atrial kick”, i.e. ventricular filling caused by atrial contraction. As shown in paper I, the notch occurs closely after rapid early filling (“E-wave” in mitral flow) but prior to ventricular filling caused by atrial contraction. A similar observation with the O-wave has also been made by PICKET and BUELL, 1993. In their work, O-wave and E/A waves are plotted simultaneously and the O-wave occurs closely at the time of the E-wave. Picket and Buell suggest that O-wave size correlates with E velocity (mitral blood flow at E-wave). The evidence that notch is seen closely after E-wave along with the fact that notch temporal position is before the P-wave in the ECG in all measurements, strongly indicates that impedance notch is caused by

early rapid ventricular filling and not by the atrial contraction. These results are supported by earlier apex cardiogram work in which it was concluded that the O-wave in the apex cardiogram is not related to mitral valve movement but more closely correlated with the peak rate of outward wall movement in early rapid filling PREWITT *et al.*, 1975. One should point out here that the impedance in question is measured on the right side, and the mitral blood flow is detected on the left side of the heart. Skeptics might say that the opening of the tricuspid valve may be later compared to mitral valve opening, and thus that tricuspid valve opening has an important role of the origin of notch. As described in chapter 3.2 on page 23, in the majority of the cases the tricuspid valve opens 23.6 ms (standard deviation 24.4 ms) before mitral blood flow as indicated in analysis of first derivative of ventricular pressures. Also, by visual inspection of the signals, as seen in Figure 3.3, the notch occurs well after indication of opening of tricuspid and mitral valve.

The notch described in the clinical data in paper I and II had similar features as the diastolic O-wave form in non-invasive transthoracic impedance data reported earlier with regards to timing and morphology. The results from paper I suggests that the notch is caused by ventricular wall movements due to the rapid early filling and not by the atrial kick. The origin of the intracardiac O-wave may possibly be an effect of ventricular wall movements caused by the rapid filling, a theory described by others (PREWITT *et al.*, 1975) but surely, more studies need to be performed to clarify the origin of intracardiac O-wave. The time between R-wave in ECG and notch (normalized with regards to average heart cycle interval) versus heart rate varied exponentially,  $r^2=0.95$ , illustrating that the notch temporal position is affected by heart rate and therefore also may be affected by ventricular filling. Bearing in mind that ventricular filling is faster during physical load due to higher venous pressure, the suggested theory in paper I also has support in the fact that timing of the notch is effected by heart rate in an exponential way as shown in paper II. One should point out, however, that the hemodynamical situation during drug induced increase of cardiac load in this study is not quite the same as in a

person who is walking or running in an upright position. In the latter case, venous return of blood to the heart is markedly increased. Even so, ventricular filling as seen with the notch is somehow affected by diastole as indicated by the notch timing versus heart rate.

As described in Table 2, the occurrence of notch in paper II varies between 80-100 % depending on inter-electrode distance and group. As for the impedance measurements only performed during resting conditions, the notch occurrence is 100% for inter-electrode distance of 20 mm, whereas it is 90 % for 10 mm and 30 mm. In the group of patients undergoing drug-induced increase of cardiac work, no such differentiation can be seen. The reason for this behavior is unknown.

In approximately 15 % of all subjects in this thesis do not present a visible notch and the reason for this can only be speculative at this point. Measurement lead tip location and ventricular apex anatomy may be important factors.

## 5.5 Summary

The intracardiac impedance notch in the present thesis has similar features with regards to temporal position as the non-invasive transthoracic impedance O-wave. The notch is observed in two different data sets; in animals and in humans and with different types of intracardiac leads (pacemaker leads in the pre-clinical study, paper I, and EP catheters in the clinical study, paper II). Several different physicians performed the lead implantation. The notch prevalence is well comparable with O-wave prevalence. With the consistent results from these two studies at hand, it can be shown that the diastolic intracardiac impedance notch is a characteristic of intracardiac impedance, and that it is a sensed physiological cardiac parameter of diastole. In addition, the notch has similar properties as the non-invasive O-wave. Since the present data is measured intracardiacly it can be concluded that the non-invasive O-wave in fact is caused by cardiac movements.



## 6 Future work

---

In future work, intracardiac impedance will be studied simultaneously with state-of-the art echocardiography using the tissue velocity imaging (TVI) technique. In TVI, the ultrasonic wave reflection signal is filtered in such a way that the movement of cardiac tissue is at focus. The cardiac tissue velocity in varying points in the heart can therefore be studied in detail. This will be performed in animals and in humans in order to further explain the origin of the notch in myocardial tissue movements.



## 7 Conclusions

---

The diastolic intracardiac impedance displays a consistent slope change called notch. The notch in the present study has similar features as the non-invasive transthoracic impedance O-wave reported earlier. The notch occurrence was found to be well comparable with results in work with O-wave reported earlier. The notch was found closely after early rapid ventricular filling but before ventricular filling caused by atrial contraction, and it is concluded that the notch is not caused by atrial contraction. The notch is most likely caused by cardiac wall movements in rapid ventricular filling.

The notch is observed in two different data sets; in animals and in humans and with different types of intracardiac leads. The lead implantation was performed by several different physicians. With the consistent results from these two studies at hand, this licentiate thesis concludes that the diastolic intracardiac impedance notch is a characteristic of intracardiac impedance, that the notch is the intracardiac equivalent of the non-invasive transthoracic impedance O-wave and that it is a sensed physiological cardiac parameter of diastole.



---

## References

---

- ALT, E., COMBS, W., WILLHAUS, R., CONDIE, C., BAMBL, E., FOTUHI, P.,  
PACHE, J., AND SCHOMIG, A. (1998): 'A comparative study of activity  
and dual sensor: activity and minute ventilation pacing responses to  
ascending and descending stairs', *PACE*, **21(10)**, pp. 1862-8
- BAAN, J., VAN DER VELDE, E. T., DE BRUIN, H. G., SMEENK, G. J., KOOPS, J.,  
VAN DIJK, A. D. TEMMERMAN, D., SENDEN, J. AND BUIS, B. (1984):  
'Continuous measurement of left ventricular volume in animals and  
humans by conductance catheter', *Circulation*, **70, No 5**, pp. 821-823
- BOONE, K., BARBER, D. C. AND BROWN, B. H. (1997): 'Review: imaging with  
electricity: report of the European Concerted Action on Impedance  
Tomography', *J. Med. Eng. Technol.*, **21** pp. 201-32
- CHARLES, R., JONES, B., AND SPINELLI, J. (1994): 'Intracardiac Impedance As a  
Rate Limit Sensor', *PACE*, **17**, pp. 852
- CHIRIFE, R. (1991): 'Sensor for right ventricular volumes using the trailing  
edge voltage of a pulse generator output', *PACE*, **14(11 Pt 2)**, 1821-7
- CHIRIFE, R., ORTEGA, D. F., AND SALAZAR, A. I. (1993): 'Feasibility of  
measuring relative right ventricular volumes and ejection fraction with  
implantable rhythm control devices', *PACE*, **16(8)**, pp. 1673-83
- DAS, G., AND CARLBLOM, D. (1990): 'Artificial cardiac pacemakers' (Review),  
*Int. J. Clin. Pharmacol. Ther. Toxicol.*, **28(5)**, pp. 177-89
- DONOVAN, K. D., DOBB, G. J., WOODS, W. PAUL D AND HOCKINGS, B. E.  
(1986): 'Comparison of transthoracic electrical impedance and  
thermodilution methods for measuring cardiac output', *Critical Care  
Medicine*, **14(12)**, pp. 1038-1044
- FOSTER, K. R., AND SCHWAN, H. P. (1989): 'Dielectric properties of tissues and  
biological materials: a critical review', *Crit. Rev. Biomed. Eng.*, **17**, pp.  
25-104

- 
- GABRIEL, S., LAU, R. W., AND GABRIEL, C. (1996): 'The dielectric properties of biological tissues: III. Parametric models for the dielectric spectrum of tissues', *Phys. Med. Biol.*, **41**, pp. 2271-2293
- HATLE, L. (1986): 'Introduction to Doppler echocardiography', *Acta Paediatr. Scand. Suppl.* **329**, pp. 7-9
- HATLE, L. (1987): 'Noninvasive measurements of intracardiac blood flow velocities with Doppler ultrasound', (Review) *Acta Med. Scand.*, **221(2)**, pp. 133-6
- HUBBARD, W. N., FISH, D. R. AND MCBRIEN, D. J. (1986): 'The use of impedance cardiography in heart failure', *Int. J. Cardiol.*, **12:1**, pp. 71-9
- KARLÖF, I. (1974): 'Haemodynamic studies at rest and during exercise in patients treated with artificial pacemaker', *Acta Paediatr. Scand. Suppl.*, **565**, pp. 1-24
- KARNEGIS, J. N., and KUBICEK, W. G. (1970): 'Physiological correlates of the cardiac thoracic impedance waveform', *Am. Heart J.*, **79:4**, pp. 519-23
- KARNEGIS, J. N., HEINZ, J., AND KUBICEK, W. G. (1981): 'Mitral regurgitation and characteristic changes in impedance cardiogram', *Br. Heart J.*, **45:5**, pp. 542-8
- KAUPPINEN, P. (1999): 'Application of lead field theory in the analysis and development of impedance cardiography', Ph.D. Thesis *Tampere University of Technology*, ISBN: 952-15-0297-5
- KELSEY, R. M., AND GUETHLEIN, W. (1990): 'An evaluation of the ensemble averaged impedance cardiogram', *Psychophysiology*, **27:1**, pp. 24-33
- KUBICEK, W. G., KARNEGIS, J. N., PATTERSON, R. P., WITSOE, D. A., AND MATTSON, R. H. (1966): 'Development and evaluation of an impedance cardiac output system', *Aerosp. Med.*, **37:12**, pp. 1208-12
- KUBICEK, W. G., KOTTKE, J., RAMOS, M. U., PATTERSON, R. P., WITSOE, D. A., LABREE, J. W., REMOLE, W., LAYMAN, T. E., SCHOENING, H., AND GARAMELA, J. T. (1974): 'The Minnesota impedance cardiography-theory and applications', *Biomed. Eng.*, **9:9**, pp. 410-6
- LABABIDI, Z. (1978): 'The O-point and diastolic impedance waveform', *Am. Heart J.*, **96:2**, pp. 277-9
- LABABIDI, Z., EHMKE, D. A., DURNIN, R. E., LEAVERTON, P. E., AND LAUER, R. M. (1970): 'The first derivative thoracic impedance cardiogram', *Circulation*, **41:4**, pp. 651-8

- LAU, C. P. (1992): 'The range of sensors and algorithms used in rate adaptive cardiac pacing' (Review), *PACE*, **15(8)**, pp. 1177-211
- MATTAR, J.A., SHOEMAKER, W.C., DIAMENT, D., LOMAR, A., LOPES, A.C., DE FREITAS, E., STELLA, F.P. AND FACTORE, L.A. (1985): 'Systolic and diastolic time intervals in the critically ill patient' *Critical Care Medicine* 1991; 19(11):1382-6
- MUZI, M., EBERT, T. J., TRISTANI, F. E., JEUTTER, D. C., BARNEY, J. A., AND SMITH, J. J. (1985): 'Determination of cardiac output using ensemble-averaged impedance cardiograms', *J. Appl. Physiol.*, **58:1**, pp. 200-5
- NICANDER, I. (1998): 'Electrical Impedance Related to experimentally induce changes of human skin and oral mucosa', *PhD thesis Karolinska Institutet* ISBN 91-628-3097-X
- NAPHOLZ, T., HAMILTON, J., AND HANSEN, J. (1990): 'Minute volume rate-responsive pacemaker', *US patent* 4901725
- NAPHOLZ, T., LUBIN, M., AND VALENTA, H. (1987): 'Metabolic-demand pacemaker and method of using the same to determine minute volume', *US patent* 4702253
- PICKETT, B. R., AND BUELL, J. C. (1993): 'Usefulness of the Impedance Cardiogram to Reflect Left Ventricular Diastolic Function', *Am. J. Cardiol.*, **71**, pp. 1099-1103
- PREWITT, T., GIBSON, D., BROWN, D., AND SUTTON, G. (1975): 'The 'rapid filling wave' of the apex cardiogram. Its relation to echocardiographic and cineangiographic measurements of ventricular filling', *Br. Heart J.*, **37**, pp. 1256-1262
- RAMOS, M. U. (1977): 'An abnormal early diastolic impedance waveform: a predictor of poor prognosis in the cardiac patient?', *Am. Heart J.*, **Vol.94, No.3**, pp. 274-281
- RHOADES, R., AND TANNER, G. (1995): 'Medical Physiology', *Little Brown* ISBN 0-316-74228-7
- SALO, R. W., PEDERSON, B. D., OLIVE, A. L., LINCOLN, W. C., AND WALLNER, T. G. (1984): 'Continuous ventricular volume assessment for diagnosis and pacemaker control', *PACE*, **7**, pp. 1267-71
- SCHALDACH, M., EBNER, E., HUTTEN, H., VON KNORRE, G. H., NIEDERLAG, W., RENTSCH, W., VOLKMAN, H., WEBER, D., AND WUNDERLICH, E. (1992): 'Right ventricular conductance to establish closed-loop pacing', *Eur. Heart J.*, **13 Suppl E**, pp. 104-12

- 
- SHOEMAKER, W. C., WO, C. C., BISHOP, M. H., APPEL, P. L., VAN DE WATER, J. M., HARRINGTON, G. R., WANG, X., AND PATIL, R. S. (1994): 'Multicenter trial of a new thoracic electrical bioimpedance device for cardiac output estimation', *Crit. Care. Med.*, **22(12)**, pp. 1907-12
- SPINELLI J. (1994): 'Continuous Hemodynamic Evaluation of The Maximum Sensor Rate' *Eur. J. Cardiac Pacing Electrophysiol.*, **2 (suppl. 4)**, pp. 202
- STAMATO, T. M., SZWARC, R. S., AND BENSON, L. N. (1995): 'Measurement of right ventricular volume by conductance catheter in closed-chest pigs', *Am. J. Physiol.*, **269**, pp. H869-H876 WOLTJER, H. H., BOGAARD, H. J., BRONZWAER, J. G., DE COCK, C. C., AND DE VRIES, P. M. (1997): 'Prediction of pulmonary capillary wedge pressure and assessment of stroke volume by noninvasive impedance cardiography', *Am. Heart J.*, **134:3**, pp. 450-5
- ZHAO T.X.. (1993): 'Electrical impedance of human blood : method and potential clinical applications', *PhD thesis at Karolinska Institutet, Stockholm 1993*, ISBN 91-628-1078-2,

---

## **Appendix**

---

### **Ethical Approvals**

UPPSALA DJURFÖRSÖKSETISKA  
NÄMND  
TIERPS TINGSRÄTT  
Box 107, 815 23 TIERP  
Tel 0293-224 70

MEDDELANDE  
1995-01-27

Bowald, Staffan  
Medical Innovation AB  
Hagby Gård  
740 10 ALMUNGE

Er ansökan nummer C 304/94 med titel 'Multipotentiell,  
multifokal, simultan defibrillering...'

Uppsala djurförsöksetiska nämnd har vid sammanträde  
95-01-27 meddelat följande

**BESLUT**

Ansökan tillstyrks. Tillståndet gäller  
95-01-27--98-01-27.

På nämndens vägnar



Adam Diamant  
sekreterare

FÖR KÄNNEDOM

UPPSALA DJURFÖRSÖKSETISKA  
NÄMND  
TIERPS TINGSRÄTT  
Box 107, 815 23 TIERP  
Tel 0293 - 224 70

MEDDELANDE  
1997-08-29

Bowald, Staffan  
Medical inov AB  
Hagby Gård  
740 10 ALMUNGE

Er ansökan nummer C 227/97 med titel 'Utredning och  
behandling av hjärtrytmier'

Uppsala djurförsöksetiska nämnd har vid sammanträde  
97-08-29 meddelat följande

**BESLUT**

Ansökan tillstyrks. Tillståndet gäller under tiden  
970829-000828.

På nämndens vägnar



Magnus Berggren  
sekreterare

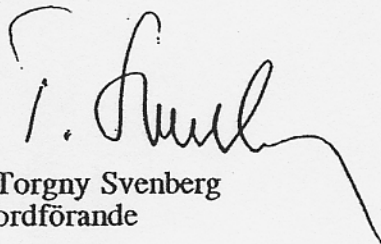


Blått

WT 0141

Ordföranden och sekreteraren i Lokal forskningsetikkommitté Nord vid Karolinska sjukhuset har 1998-02-16 granskat nedanstående projekt.

Dnr	Sökanden	Beslut
97-152	Böl Börje Darpö, kardiologklin, KS Forskningsing Karin Järverud, Pacesetter AB, Solna  Titel: Akut impedansmätning i höger kammare i vila och under farmakologisk stress på patienter som genomgår elektro- fysiologisk undersökning.	De till lokala forskningsetikkommittén Nord vid Karolinska sjukhuset insända komplette- ringarna har granskats och godkänts.

  
Torgny Svenberg  
ordförande

  
Karin Schenck-Gustafsson  
sekreterare

---

# Paper I

Analysis of the O-wave in acute right ventricular apex impedance  
measurements with a standard pacing lead in animals

Karin Järverud, Stig Ollmar, Lars-Åke Brodin

Medical and Biological Engineering and Computing (Med. & Biol.  
Eng. Comput.), 2002, **40(5)**, pp. 512-519

---

## **Paper II**

Analysis of O-wave in acute right ventricular apex impedance in  
humans (manuscript submitted)

Karin Järverud, Börje Darpö, Lars-Åke Brodin, Stig Ollmar